Accepted Manuscript

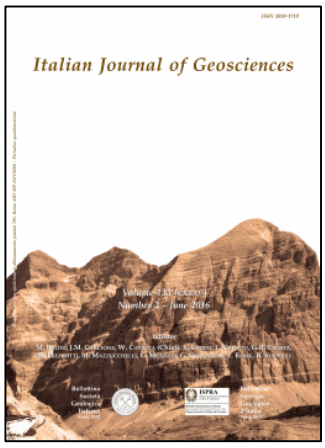

Styles and rates of deformation in the frontal accretionary wedge of the Calabrian Arc (Ionian Sea): controls exerted by the structure of the lower African plate

Bortoluzzi G., Polonia A., Torelli L., Artoni A., Carlini M., Carone S., Carrara G., Cuffaro M., Del Bianco F., D'Oriano F., Ferrante V., Gasperini L., Ivaldi R., Laterra A., Ligi M., Locritani M., Muccini F., Mussoni P., Priore F., Riminucci F., Romano S., Stanghellini G.

To appear in: *Italian Journal of Geosciences*

Received date: 15 June 2016

Accepted date: 13 September 2016

doi: 10.3301/IJG.2016.11

Please cite this article as:

Bortoluzzi G., Polonia A., Torelli L., Artoni A., Carlini M., Carone S., Carrara G., Cuffaro M., Del Bianco F., D'Oriano F., Ferrante V., Gasperini L., Ivaldi R., Laterra A., Ligi M., Locritani M., Muccini F., Mussoni P., Priore F., Riminucci F., Romano S., Stanghellini G. - Styles and rates of deformation in the frontal accretionary wedge of the Calabrian Arc (Ionian Sea): controls exerted by the structure of the lower African plate, *Italian Journal of Geosciences* 10.3301/IJG.2016.11

Styles and rates of deformation in the frontal accretionary wedge of the Calabrian Arc (Ionian Sea): controls exerted by the structure of the lower African plate.

Bortoluzzi G. (1), Polonia A. * (1), Torelli L. (2), Artoni A. (2), Carlini M. (2), Carone S. (3), Carrara G. (1[a]), Cuffaro M. (4), Del Bianco F. (1[b]), D'Oriano F. (1[a]), Ferrante V. (1), Gasperini L. (1), Ivaldi R. (3), Laterra A. (3), Ligi M. (1), Locritani M. (5), Muccini F. (5), Mussoni P. (2[d]), Priore F. (1[b]), Riminucci F. (1[b]), Romano S. (1), Stanghellini G. (1)

*: corresponding author
1- Institute of Marine Science CNR ISMAR-Bo, Via Gobetti, 101, 40129 Bologna, Italy
Tel: +39 051-6398888, e-mail: alina.polonia@ismar.cnr.it
2- Department of Physics and Earth Sciences, University of Parma, Parco Area delle Scienze, 157/A, Parma
3- Istituto Idrografico della Marina, Passo Osservatorio, 4 -16134 – GENOVA
4- Istituto di Geologia Ambientale e Geoingegneria, CNR, c/o Dipartimento di Scienze della Terra, Sapienza Università di Roma, P.le A. Moro 5, I-00185 Rome, ITALY
5- Istituto Nazionale di Geofisica e Vulcanologia, via di Vigna Murata 605, 00143 Rome, Italy

a now: independent researcher
b now: PROAMBIENTE S.c.r.l., Emilia-Romagna High Technology Network, Via P. Gobetti, 101 40129, Bologna, Italy
d now: Eni S.p.A.- Upstream and Technical Services (GEOS)

Abstract

The Calabrian Arc is a narrow subduction-rollback system resulting from Africa/Eurasia plate convergence. We analysed the structural style of the frontal accretionary wedge through a multi-scale geophysical approach. Pre-stack depth-migrated crustal-scale seismic profiles unravelled the overall geometry of the subduction complex; high-resolution multi-channel seismic and sub-bottom CHIRP profiles, together with morpho-structural maps, integrated deep data and constrained the fine structure of the frontal accretionary wedge, as well as deformation processes along the outer deformation front.

We identified four main morpho-structural domains in the western lobe of the frontal wedge: the proto-deformation area at the transition with the abyssal plain; two regions of gentle and tight folding; a hummocky morphology domain with deep depressions and intervening structural highs; a highstanding plateau at the landward limit of the salt-bearing accretionary wedge, where the detachment cuts through deeper levels down to the basement. Variation of structural style and seafloor morphology in these domains are related to a progressively more intense deformation towards the inner wedge, while abrupt changes are linked to inherited structures in the lower African plate. Our data suggest focusing of intense shallow deformation in correspondence of deeply rooted faults and basement highs of the incoming plate.

Back-arc extension in the Southern Tyrrhenian Sea has recently ceased, producing a slowdown of slab rollback and plate-boundary re-organization along trans-tensional lithospheric faults segmenting the continental margin. In this complex setting, it is not clear if the accretionary wedge is still growing through frontal accretion. Our data suggest that shortening is still active at the toe of the wedge, and uplift rates along single folds are in the range of 0.25-1.5 mm/yr. An unconformity within the Plio-Quaternary sediments suggests a discontinuity in sedimentation and tectonic processes, i.e. a slowdown of shortening rate or an increase in sedimentation rate, but not a real inactivation of frontal accretion, which still contributes to the migration of the outer deformation front towards the foreland.

Introduction

The Calabria Arc (CA) is a narrow and arcuate subduction-rollback system characterized by a thickly sedimented lower African plate and an irregular plate boundary reflecting the presence of continental blocks, indenters, and different rates of continental collision. The subduction complex is the result of the southeastward retreat of the Tethyan slab during the last 35–30 Ma (Rehault et alii, 1984; Malinverno and Ryan, 1986; Gueguen et al., 1998; Jolivet and Faccenna, 2000; Faccenna et al., 2001a, 2004; Rosenbaum and Lister, 2004), back-arc extension in the Tyrrhenian Sea since ~10 Ma (Malinverno and Ryan, 1986; Faccenna et alii, 2001b) and the formation of the Aeolian island arc. It shows a composite structure reflecting interaction of crustal blocks along an irregular plate boundary and the interference between different tectonic domains: (i) the Tyrrhenian back arc basin and the volcanic arc to the North; (ii) two buoyant continental lithospheric blocks, i.e. the Malta-Iblean plateau to the West and Apulia platform to the East, bounding laterally the subduction system; (iii) the forearc region dominated by underplating and offscraping processes and crustal scale margin segmentation; (iv) the foreland region to the South-East marked by the presence of topographic highs and varying structure of the incoming plate; v) the Hellenic subduction system to the SE.

In the forearc region, a 300 km wide accretionary wedge (Finetti et alii, 2005; Cernobori et alii, 1996; Doglioni et alii, 1999a; Minelli and Faccenna 2010; Polonia et alii, 2011; Gallais et alii, 2012) records recentmost convergence processes and shows very fast rates of outward growth since Messinian times (Polonia et alii, 2011). The accretionary complex is segmented both along and across strike, and this has been related to various tectonic processes, and different rates of plate coupling on the subduction interface. Moreover, transfer tectonics along major NW-SE lithospheric features have been described as the shallow expression of slab tearing and plate boundary re-organization during Pleistocene (Polonia et alii, 2016a). The transition between the CA accretionary complex and the African foreland occurs at the toe of the frontal wedge, where an abyssal plain is still present (Fig. 1). The Ionian basin is one of the Eastern Mediterranean domains with “Tethyan

affinity", together with the Sirte and Herodotus deep basins, and it marks the western boundary of the Hellenic subduction system (Fig. 1).

In this paper, we combine high penetration multichannel seismic reflection profiles, gravity data and multibeam maps collected in the frontal part of the CA subduction system to describe: a) shallow deformation of the frontal accretionary wedge; b) structure of the underplating African crust; c) the interplay between active tectonics and deeply rooted features in the lower plate. Our analyses aims to understand if the wedge is still growing or if its activity is ceased recently and if structural development is influenced by the structure of the lower plate.

2.0 – Tectonic setting

The Calabrian Arc subduction complex is the result of Africa Eurasia plate convergence, presently occurring at the very slow rate of about 5-7 mm/yr (De Mets et alii, 1994; Hollenstein et alii, 2003; Serpelloni et alii, 2007; D'Agostino et alii, 2008; Devoti et alii, 2008) and slab rollback in the backarc region (Malinverno and Ryan, 1986; Faccena et alii, 2004; Doglioni et alii, 1999b, which produced the 1200 km displacement of Calabria (Bonardi et alii, 2001; Faccenna et alii, 2001a; Barberi et alii, 2004; Rosembaum and Lister, 2004) during the opening of the Liguro-Provencal (35-16 Ma) and the Tyrrhenian (12 Ma – present) basins (Patacca et alii, 1990; Gueguen et alii, 1998; Faccenna et alii, 2001b; Rosembaum et alii, 2002; Nicolosi et alii, 2006).

Recent GPS measurements suggest a small amount of E-W extension in the Tyrrhenian basin (Serpelloni et alii; 2007). Trench retreat was particularly fast over the Neogene and early Quaternary (Patacca et alii, 1990) as indicated by high extension rates (50-70 mm/yr) recorded in the Tyrrhenian oceanic seamounts (*Marani and Trua*, 2002; *Mattei et alii*, 2002) and rapid migration of the trench (Faccenna et alii, 2001). On the other hand, vertical axis rotations responsible for the arcuate shape of the CA occurred during Miocene to Quaternary but were almost finished 1 Ma (*Mattei et alii*, 2007) as confirmed by GPS results showing no active back-arc extension in the Southern Tyrrhenian Sea (D'Agostino et alii, 2008).

Despite the very slow modern-day plate convergence rates observed by GPS, shortening is still active in the CA, as outlined by incipient deformation observed in different portions of the accretionary wedge (Polonia et alii, 2011 and 2012). GPS vectors of Calabria relative to Apulia motion show systematic residuals directed towards the Ionian Sea suggesting an outward motion of the CA with shortening taken up in the accretionary wedge (D'Agostino et alii, 2008).

In the submerged subduction complex, five main morpho-structural domains have been identified (Fig. 2) from SE to NW: 1) the abyssal plain which is possibly characterized by the oldest in situ fragment of oceanic crust in the world even though its nature is highly debated (Speranza et al., 2012 and references therein); 2) the post-Messinian accretionary wedge; 3) a slope terrace; 4) the pre-Messinian accretionary wedge; and 5) the inner plateau. Variation of structural style and seafloor morphology in these domains are related to different tectonic processes, including frontal accretion, out-of-sequence thrusting, underplating and complex faulting.

Along strike segmentation of the continental margin has produced two different lobes of the accretionary wedge with very different structural setting and geometry (Polonia et alii, 2011). The Western Lobe (WL), offshore the Messina Straits region, shows an accretionary wedge bounded towards the continent by a slope terrace that is the site of a Messinian thrust-top basin. This basin develops in the region where the basal detachment cuts through deeper levels down to the basement and where out-of-sequence thrust faults develop to accommodate basal detachment depth variations. The frontal part of the Western lobe detaches on the base of Messinian evaporites and the associated thin-skinned tectonics produces a very low tapered (taper < 1.5°) salt-bearing accretionary wedge (Fig. 3a). The Eastern Lobe (EL), in front of Central Calabria, shows a different structure (Fig. 3b), with a more elevated wedge (500-600m shallower), characterized by steeper slopes and higher deformation rates. This is reflected in a different structural style and thrust faults that involves the basement (thick skinned tectonics) in the frontal part of the accretionary wedge. The migrating Calabria trench drives the entire accretionary wedge outward, but the two lobes of the wedge experience different boundary conditions: the EL collides with the Mediterranean Ridge, whereas

the WL is free to spread into the Ionian abyssal plain. The EL and WL are delimited by the Ionian Fault system (IF), a NW-SE deformation zone (Fig. 2) crossing the entire subduction complex from the abyssal plain to the Messina Straits.

Seismic data reveal that the subduction complex is segmented also within the WL, along a NNW-SSE trending active crustal fault named Alfeo-Etna fault system (AEF) by Polonia et alii, (2016a) and described by other authors in the past (Nicolich et alii, 2000; Rosembaum et alii, Argnani et alii, 2008; Polonia et alii, 2011; Polonia et alii, 2012; Gallais et alii, 2013; Gutscher et alii, 2016).

Analysis of multichannel seismic reflection profiles shows that the IF and the AEF are transfer crustal tectonic features bounding a complex deformation zone, which produces the downthrown of the WL along a set of poliphased transtensive fault strands. During Pleistocene, transtensive faulting reactivated structural boundaries inherited from the Mesozoic Tethyan domain, which presently accommodate a recent tectonic re-arrangement coeval and possibly linked to the Mt. Etna formation. Regional geodynamic models show that, whereas AEF and IF are neighboring tectonic systems, their individual roles are different. The IF accommodates, along its NW sector, deformation primarily resulting from the ESE retreat of the Ionian slab. On the other hand, the AEF is part of the overall dextral shear deformation resulting from differences in the Africa-Eurasia motion between the western and eastern sectors of the Tyrrhenian margin of northern Sicily (Polonia et alii, 2016a). It thus accommodates diverging motions in the adjacent compartments, which result in rifting processes within the WL of the Calabrian Arc accretionary wedge. As such, it is primarily associated with Africa-Eurasia relative motion which causes the segmentation of the Neogene accretionary wedge.

In the following sections, we will describe in detail the frontal part of the WL through the analysis of seismic reflection profiles at different scales, with the main purpose of understanding whether margin segmentation is active in the frontal part of the system and if shortening is still active along the plate boundary. Moreover, we will try to investigate the deeply rooted structures on

the incoming plate, to see whether they are related to the composite nature of the incoming plate and whether this complex setting controls active deformation in the accretionary wedge.

3.0 - Methods

To resolve active tectonics at the front of the subduction system we carried out a combined interpretation of seismic reflection profiles at different scales.

Deep penetration multichannel seismics. Deep penetration seismic profiles (CNR_ENI Deep Crust Seismic Profiles – CROP) were used to reconstruct the overall geometry of the subduction complex, i.e., depth of the basal detachment, top of the African basement and deep structure of the incoming plate. We obtained full pre-stack depth-migrated (PSDM) seismic sections, through an iterative migration procedure (the SIRIUS/GXT, Migpack software package), that uses seismic velocities constrained by focusing analysis and common reflection point gathers. Other deep penetration seismic lines (Mediterranean Sea MS dataset collected by OGS) have been used to define geometry and extent of deep structures in the Ionian Sea abyssal plain.

High resolution multichannel seismic lines have been used to define the structural style in the different domains of the outer accretionary wedge. MCS profiles were collected using an array of 2 SERCEL G.I. guns as seismic source, and a 48 channels, 1200 m-long streamer as receiver. Seismic data processing includes preliminary velocity analysis, Dip Move Out (DMO), velocity analysis after DMO, stack and time migration.

Sub-bottom CHIRP data: We used these data to study active deformation in the shallow sub-surface. Seismic data has been acquired with a Benthos CHIRP-III sonar system operating with 16 hull-mounted transducers (3-7 KHz sweep frequency) and processed using SeisPrho software (Gasperini and Stanghellini, 2009), applying time variant gain, automatic gain control and band – pass filters.

Multibeam data were acquired during two cruises in 2007 and 2009 with R/V OGS Explora equipped with a Reson 8150 multibeam system (234 beams, 12 kHz) and positioning provided by

GPS Ashtech Acquarius. Sound profiles were performed using the Reson Navitronic sound velocity profile (SVP) 25.

4.0 Data analyses

Three seismic lines orthogonal to the outer deformation front are analysed from East to West. They highlight structural variations across the plate boundary suggesting the subdivision of the frontal portion of the subduction complex in different seismo-tectonic provinces, characterized by rather homogeneous structural style, deformation rate, basal detachment and basement depth. Structural boundaries between seismo-tectonic domains are marked by abrupt variation of these characters. Seismic lines were selected among the whole CALAMARE dataset as the most representative of these provinces. One tie MCS line, roughly parallel to the foredeep (MS-112) is then described, to address along strike structural and stratigraphic variations. Finally, a morphobathymetric high-resolution multibeam map is used to connect shallow morphotectonic setting of these domains and analyse the shallow expression of their boundaries.

4.1 Multichannel seismic lines

4.1.1 – Seismic line CALA 05 (Figs. 4 and 5)

This line crosses the subduction complex in the westernmost study region (Fig. 2), close to the Malta escarpment and the Medina seamount.

- Abyssal plain (s.p. 100 - 580). The relatively undeformed abyssal plain domain allows good seismic penetration and deep reflector imaging down to the basement (about 8.5 s TWT). The Mesozoic carbonates are 3.5 s (TWT) thick, while the Tertiary section is only 200 ms (TWT) thick. Messinian evaporites are relatively undeformed (Fig. 5a) and about 2000 m thick (0.5 s TWT) while Plio-Quaternary (P-Q) sediments resting on the evaporites are made of a succession of sediment drifts (Fig. 5b) possibly related to bottom currents controlled by prominent topography.

- Accretionary wedge (s.p. 580-end of line): The wedge is bounded by the outer deformation front, which is located where the outermost fold affects the seafloor morphology (s.p. 580). The blow-up in Fig. 5a shows a cumulative deformation producing a progressive increase in fold amplitude in deeper layers. Two piggy back basins are controlled by the outermost folding processes. As the outer deformation front is approached the P-Q and Messinian units are shortened and uplifted along tight folds bounded by landward dipping thrust faults soling out on the base of the Messinian evaporites which acts as the basal detachment. Fold amplitude increases also moving towards the inner portions of the accretionary wedge. Within the wedge, deformation is rather homogenous and no major structural variations are imaged. In the outer part of the accretionary wedge both landward and seaward structural vergence is present while from s.p. 1500 the seaward vergence prevails.

4.1.2 – Seismic line CALA-04 (Figs. 6 and 7)

In this MCS line, the outer wedge shows a step like morphology with three topographic scarps delimiting rather flat regions. Five domains are imaged in line CALA-04:

- Abyssal plain (s.p. 2980 - end of line). Deep reflectors down to the basement at about 8.5 s TWT are well imaged. The P-Q sediments are 400 ms thick on average (about 400 m), while the Messinian evaporites are about 500 ms thick (about 1000 m). Tertiary and Mesozoic sediments, about 1500 m and 3500 m thick respectively, show deformation along S-ward dipping thrust faults which possibly re-activate previous normal faults bounding crustal blocks, as imaged in seismic line M-2B (Fig. 3a). This tectonic uplift affects the base of the Messinian evaporites (see s.p. 3400-3450). The abyssal plain is bounded towards NW by the outer deformation front (s.p. 2980), where the outermost deformation affecting the seafloor is visible. At s.p. 3030, close to the deformation front, an incipient fold deforms the entire sedimentary section without affecting the seafloor (proto-deformation). Seaward of this point (s.p. 3030-3120), deformation does not reach up to the seafloor, but rather stops at a major unconformity present at about 200 ms TWT b.s.f.. Below this unconformity, deformation is related to wide folding, which shorten and uplift the top of the

Messianian evaporites too; above, sediments in the abyssal plain are less deformed, while in the proto-deformation zone the unconformity is uplifted above the growing fold at s.p. 3030 (Fig. 7a). Chirp profile in Figure 7b displays a succession of turbidite beds filling the abyssal plain. The recentmost of these megabeds is the HAT (Homogenite/Augias turbidite), emplaced after the A.D. 365 Crete earthquake and tsunami (Polonia et alii, 2013), while the deeper megaturbidite is the Deep Transparent Layer (DTL) of Hieke (2000), whose age, reconstructed through ^{14}C dating, is about 14,000 yr b.p. (Polonia et alii, 2013). This implies that about 30 m of sediments were deposited during the last 14,000 yrs, suggesting a relative high sedimentation rate for this abyssal environment. Below the DTL, a third megabed is visible, the TTL (Thick Transparent Layer) of Hieke (2000).

- **Outer wedge, gentle deformation** (s.p. 2730-2980, Figs. 6 and 7a). Sediments are uplifted landward of the deformation front. This part of the accretionary wedge shows very low taper, gentle folding and a rather thick P-Q sediment section. Landward dipping reflectors, topographic breaks of the seafloor and offset of deeper reflectors, suggest the existence of thrust faults. Morphological breaks (s.p 2730 and 2900, Fig. 6) and alternating sedimentary basins develop above a deeply rooted fault system, which produces displacement in the Tertiary and Mesozoic sediments and uplift of the basement.

- **Outer wedge, tight deformation** (s.p. 2540-2730). Here, short wavelength and low amplitude folding affects P-Q sediments as well as upper Messinian evaporites. This sector is bounded by two morphological breaks (Fig. 6).

- **Outer wedge, rough topography** (s.p. 2070-2540, Fig. 6). A number of V-shaped troughs and box shaped depressions, up to 250 m deep, are present, producing a very rough morphology of the seafloor, with Messinian salt possibly outcropping at the seafloor. This peculiar morphology is associated with disruption of deep reflectors.

- **Outer wedge, highstanding plateau** (s.p. 1320-2070, Fig. 6). This is a rather flat area, with a relatively less deformed seafloor. The basal detachment is present at about 6.3-6.5 s (TWT), while

high amplitude and sub-horizontal deep reflectors are imaged down to the basement, located at about 8.3 s TWT. This domain is bounded towards the continent by a slope terrace which hosts the out-of-sequence thrust fault Splay-1 (Fig. 2), developing at the transition between the salt-bearing post-Messinian accretionary wedge, and the pre-Messinian wedge detaching on a deeper level (see Fig. 3a for correlation).

4.1.3 – Seismic line CALA-15 (Figs. 8 and 9)

This profile was collected in the eastern region of the WL and is close and parallel to the CROP seismic line M-2B (Figs. 2 and 3a).

- Abyssal plain (s.p. 1670 - end of line, Fig. 8). Deep reflectors, down to the basement at about 8.2 s TWT, are well imaged. The thickness of P-Q sediments ranges between 300 and 500 ms TWT (about 300-500 m), while the Messinian evaporites are 700 ms thick on average (about 1400 m). Tertiary and Mesozoic sediments (about 1 s TWT and 0.8 s TWT respectively) are affected by progressive deformation along S-ward dipping reverse faults, as imaged in seismic line M-2B (Fig. 3a). The abyssal plain is bounded towards NW by the outer deformation front (s.p. 1670), where the first fold affecting the seafloor is visible on the MCS line. However, seaward of the deformation front, the top of the Messinian evaporites and the Plio-Quaternary sequence are folded and uplifted, even though deformation does not reach the seafloor. A major unconformity is present at about 250 ms TWT b.s.f. (Fig. 9a). Below this unconformity, deformation is related to large wavelength folding, while uppermost sediments are less deformed and show only weak undulations. In the proto-deformation zone (s.p. 1700-1800, Fig. 9b) the unconformity is also uplifted above growing folds, as evidenced by the Chirp profile in Fig.6c, which images a succession of deformed megabeds (HAT, DTL and TTL) filling the abyssal plain. The HAT is about 18 m thick, while the DTL is 8 m thick providing a very high sedimentation rate during the Holocene.

- Outer wedge, gentle deformation (s.p. 1670-1520, Fig. 8). Sediments are uplifted due to gentle folding. Landward dipping reflectors, sediment disruption and displacement of deeper reflectors,

suggest the existence of thrust faults. Opposite verging folds and wide sedimentary basins, develop in this region, which appears to be in continuity with the abyssal plain. This domain is bounded towards the continent by a morphological break at s.p. 1520 (Figs. 8 and 9a).

- Outer wedge, tight deformation (s.p. 1520-1220, Fig. 8). As s.p. 1520 is approached, short wavelength and low amplitude tight folding affects P-Q sediments, as well as upper Messinian evaporites. This domain develops above a basement high, and deep faults which deform Mesozoic and Tertiary sediments. Thrust faults within the post-Messinian accretionary wedge sole out on the base of the Messinian evaporites.

- Outer wedge, rough topography (s.p. 1220-500, Fig. 8). A number of V-shaped troughs and box shaped depressions, up to 250 m deep, are associated with a rough morphology of the seafloor. Major depressions, where Messinian evaporites appear to outcrop at the seafloor, develop above deep faults, suggesting that the two occurences, i.e. rough topography and deeply rooted deformation, are somehow related.

- Outer wedge, highstanding plateau (s.p. 1320-2070, Fig. 8). This is a rather flat area, with a relatively undeformed seafloor. The basal detachment is present at about 6.2-6.3 s (TWT), while high amplitude and sub-horizontal deep reflectors are imaged down to the basement, located at about 8.0 s TWT.

4.1.4 – Seismic line MS-112 (Fig. 10)

This E-W trending profile crosses all seismic lines described in the previous sections and provides a complete longitudinal section of the WL, which could be used to check whether margin segmentation processes are active at the frontal wedge. Three major crustal discontinuities, CD1, CD2, and CD3 are visible in this seismic profile (Fig. 10). CD1 is located at the western deformation front, where frontal wedge thrust faults displace the seafloor; these faults are associated, but apparently not directly linked, to deep sub-vertical faults, which produce tilting and displacement of seismic reflectors down to the basement. The second set of sub-vertical crustal

faults (CD2) are located at s.p. 1400. Seismic reflectors appear to be disrupted along such structural boundary, even though they do not show vertical throws, suggesting prevalent strike-slip deformation. This region is on the seaward extension of the Alfeo-Etna fault system (Fig. 2), and thus may represent a propagation of this fault in the frontal wedge, despite deformation is weaker than in the inner domain (see for example Fig. 8 in Polonia et alii, 2016a). A wide region of crustal deformation is present between s.p. 1800 and 2100 (CD3 in Fig. 10), where the seafloor shows a very rough topography with large depressions and intervening structural highs. Seaward of this region the Tertiary and Mesozoic sediments are uplifted, tilted and deformed along seaward dipping faults as imaged in seismic line CROP M-2B (Fig. 3a). The basal detachment, i.e., the base of the Messinian evaporites, is slightly deformed along these tectonic features. The progression of structural domains within the frontal wedge (gentle and tight deformation, rough morphology and high-standing plateau) is well imaged in the eastern part of the profile, which crosses the eastern part of the frontal wedge. The basal detachment at the base of the Messinian evaporites is located at a depth between 6 and 6.5 s TWT; above the detachment, the salt-bearing accretionary wedge shows a chaotic seismic facies, while older sedimentary units, represented by well layered seismic reflectors down to the basement (purple reflector in Fig. 10), are underthrusted below the basal detachment. The seaward boundary of the rough morphology domain is clearly located where the basement high and deep faults are imaged (Fig. 10).

4.2 – Multibeam data

High-resolution multibeam data highlight the fine morpho-structural setting of the frontal wedge, which is dominated by a corrugated pattern of small-scale folds and depressions aligned parallel to the isobaths (Fig. 11). The transition between the flat, relatively undeformed abyssal plain and the accretionary wedge is marked by the inception of small wavelength folds, which appear to be rather discontinuous. The frontal wedge shows two lateral ramps (LR1 and LR2 in Fig. 11), that displace left-laterally the outer deformation front, and are associated with NE-SW lineaments within the

accretionary wedge. These lineaments are marked in the seismic line CALA 04 by seafloor scarps (s.p. 2900 and 2730, Fig. 6). The NW/SE morpho-tectonic lineaments develop in sectors where MCS lines show evidence of deep faulting and basement highs (Figs. 6, 8, and 10).

Short and overlapping folds, whose trend follow the arcuate external shape of the WL (Fig. 11), represent the gentle deformation domain. The tight deformation domain, given by even shorter wavelength folds, is bounded towards NW by a very rough morphology represented by elongated and anastomosing depression and structural highs. This domain widens towards East where it reaches its maximum width as evidenced in the MCS lines (Figs. 4, 6, 8 and 10). To the East, the intervening structural highs between the depressions are wider (Fig. 11). On the other hand, in the western region (seismic line CALA 05, Fig. 4) this domain appears very narrow and represented by two isolated depressions between s.p. 1400 and 1500 (Fig. 4). The innermost high standing plateau is a rather flat domain where elongated depressions are less frequent (red area at about 3200-3500 m depth in Fig. 11).

5.0 Discussion

Post-Messinian frontal accretion in the WL has produced a salt-bearing accretionary wedge with a very peculiar geometry and structural setting. The very low taper angle (about 1-1,5°) is mainly related to the rheology of evaporites, which provide a very weak basal detachment enhancing high rates of outward growth of the accretionary complex towards the foreland. On the other hand, recent margin segmentation processes along lithospheric transtensive fault systems have produced the downthrown of the western accretionary wedge and rifting perpendicular to the trench axis along the Ionian and Alfeo/Etna fault systems (Polonia et alii, 2016a). This complex setting may be related to a Middle Pleistocene tectonic reorganization in the central Mediterranean driven by the stalling of the Calabrian roll-back/subduction and related Tyrrhenian back-arc extension (Wortel and Spakman, 2000; Goes et alii, 2004; Faccenna et alii, 2011). Several crustal expressions, including the partial jump of the Sicilian thrusting towards the southern Tyrrhenian contractional

belt, and the triggering of Mt. Etna volcanism (Gvirtzman and Nur, 1999; Doglioni et alii, 2001; Faccenna et alii, 2011; Polonia et alii, 2016a) are probably among the major consequences of such processes. Given the complex tectonic setting, characterized by different stress fields acting together, and considering that the CA is close to continental collision, it is not clear whether the Africa/Eurasia plate convergence is still driving shortening in the frontal wedge or the wedge is presently inactive. The combined interpretation of MCS lines and multibeam data in the frontal part of the subduction-rollback system provides new insights to address this issue.

5.1 Summary of tectonic domains in the frontal accretionary wedge

Analyses of MCS lines in the frontal wedge suggests the progression of different tectonic domains characterized by varying structural styles and morpho-bathymetric features. The flat and relatively undeformed abyssal plain is filled by turbidites and thick megabeds, while close to the Malta escarpment bottom currents cause the formation of prominent contourite drifts (Fig. 5b). As the deformation front is approached, the P-Q and Messinian sediments resting on the African plate are shortened and uplifted along fault-controlled folds. Thrust faults sole out on the base of the Messinian evaporites and generally breach through the Plio-Quaternary sedimentary section displacing the seafloor (see s.p. 970 in Fig. 4). Moving from the outer deformation front, towards the inner parts of the frontal wedge, progressive deformation produces more intense sediments disruption and tectonic uplift. In the western domain (line CALA 05, Fig. 4) the frontal wedge shows a rather uniform slope with taper of about 1°, while in the central and eastern sectors (lines CALA 04 and CALA 15, Figs. 6 and 8) structural changes are more abrupt. Here, the frontal wedge shows three main domains, characterized by gentle folds, tight folding and a succession of deep depressions and structural highs (rough topography domain), respectively. The high-standing plateau represents the transition to the slope terrace (Figs. 3a and 6), which is the site of out-of-sequence thrust faults developing at the transition with the pre-Messinian inner wedge, where the detachments cuts through deeper levels down to the basement.

5.2 Structure of the lower African plate

MCS line MS-112 (Fig. 2) suggests that the Alfeo-Etna fault system did propagate in the frontal part of the wedge, but deformation rates are lower than in the region to the North and no sedimentary basin develops along the fault in this region. This would imply that the fault has propagated recently, or that it dies out in the frontal wedge. On the other hand, the prominent rough morphology domain of the frontal wedge, characterized by the presence of alternating structural highs and deep troughs, appears related to the presence of deeply rooted structures (Fig. 10, s.p. 1800-2100). NW and SE of this region, below the accretionary complex, which is detaching on the base of evaporites located between 6.2 and 6.5 s TWT, Tertiary and Mesozoic sediments are characterized by high-amplitude and sub-horizontal layering. In the rough morphology domain, the basal detachment is discontinuous, and no coherent reflectors are visible below the evaporites. The rough topography domain is bounded towards the SE by Tertiary and Mesozoic seaward dipping reflectors and a prominent basement high (Figs. 3a, 6, 8, 10).

Analysis of all available MCS lines suggests that the top of the basement in the abyssal plain is located at a rather constant depth (about 8.2 s TWT). It appears uplifted and displaced by 0.8-1 s TWT along a sub-vertical fault below the frontal wedge (Fig. 3a s.p. 200-800, Fig. 8 s.p. 1200-1300 and Fig. 10 s.p. 2000-2400). On the other hand, the thickness of Mesozoic and Tertiary sediments varies across strike. The base of Tertiary sediments is 1.5 s TWT deeper to the East (line CALA 15, Fig. 8) relative to the western region, and the same is true for the base of the Messinian sediments. This implies that thicker Tertiary and Messinian basins were present in the eastern part of the WL closer to the Ionian Fault.

In this region, the basement high shows its maximum uplift as evidenced by MCS lines. These observations suggest that the deep structure of the incoming plate is probably inherited since Mesozoic times. We thus propose that the discontinuity bounding the rough topography domain may represent a major Mesozoic paleoceanographyc boundary.

The deep structure of the lower African plate is controlling structural development within the accretionary wedge. Subduction of the basement topography and related faults on the lower plate may have played a role in the shallow structure possibly triggering fluid flow, dissolution of evaporites and recent sediment deformation. The rough seafloor morphology of the Calabrian Arc accretionary wedge was termed "cobblestone topography" (*Hersey*, 1965; *Kastens and Cita*, 1981; and *Rossi and Sartori*, 1981) and interpreted as due to collapse structures driven by karst processes (*Hinz*, 1972; *Ryan, Hsu et alii*, 1973) or by a combined effect of tectonics and salt diapirism (*Kastens*, 1981; *Camerlenghi and Cita*, 1987). Our data suggest that these surficial features appears to be controlled by deeply rooted faults and basement highs on the incoming plate. Subduction or underplating of lateral morphological or rheological heterogeneities affects upper plate and may produce structural disruption, tectonic erosion as shown in other setting (Lallemand et al., 1992). The basement high and deep faults below the accretionary wedge as imaged by seismic line CALA 05 (Fig. 4), CALA 15 (Fig. 8) and CROP M2B (Fig. 3a) clearly show that have affected sediment disruption within the accretionary wedge despite it is sealed by sediments.

5.3 The Calabrian Arc and the Kephalonia fault system

The complex structural development in the frontal part of the CA accretionary wedge is the result of the overall Africa/Eurasia plate convergence. However, its location close to the Hellenic Arc makes this region accommodating deformation processes of both subduction systems and, more importantly, their lateral boundaries. Let us consider the structural control exerted by the segmented Calabrian and Hellenic Arcs on the frontal accretionary wedge in the Ionian Sea.

Margin segmentation in the CA occurs along the AEF and IF systems in the WL of the accretionary wedge. Active deformation along such major transverse faults suggests a transtensional motion associated with a complex deformation pattern of strike-slip and normal faulting, which give rise to the formation of sedimentary basins, ridges and morphological scarps (Polonia et alii, 2016a). Seismo-stratigraphic analysis reveals that transtensional faulting along the AEF and IF

systems re-activates Mesozoic features located in the lower African plate. They could be oceanic fracture zones of the Tethyan domain, whose orientation is compatible with the NW-SE fault direction (Frizon de Lamotte et alii, 2011). These major boundaries acted as paleo-oceanographic boundaries during the Messinian salinity crisis and are presently accommodating plate boundary re-organization. Tearing processes at the slab edge in the Messina Straits region and the collision of the CA with the Mediterranean Ridge (Fig. 2) are accommodated along the IF system (Polonia et alii, 2016a) and causes segmentation of the subduction complex in two lobes (WL and EL, Fig. 2). The EL is characterized by thick skinned tectonics along an imbricate fault structure (Fig. 3b) which produces an accretionary wedge more similar to a fold and thrust belt (Polonia et alii, 2011). The WL shows a very wide (300 Km) and very low tapered accretionary wedge still free to move towards the foreland (Fig. 3a).

The active Hellenic subduction front to the East, is dextrally offset by 100 –120 km across the Kephalonia Transform Zone, coinciding with the junction of a slowly subducting Adriatic continental lithosphere in the north and a rapidly subducting Ionian oceanic lithosphere in the south (Royden and Papanikolau, 2011). Pliocene differentiation of the Hellenides and formation of the Kephalonia transform are the direct result of oceanic lithosphere of the Ionian Sea entering the trench south of Kephalonia while continental lithosphere continued to be subducted north of the trench (Royden and Papanikolau, 2011; Bradley et alii, 2013). The frontal CA accretionary wedge is located in a region where the foredeeps, the NW-SE transtensive faults of the CA and the Kephalonia fault system connect and interfere in a sort of triple junction. We propose that the deep structure of the frontal accretionary wedge with deep faults soling out below the uplifted basement is the result of basement-involved tectonic processes controlled by the paleoceanography of the Tethyan ocean and by recent (Pleistocene) processes driven by collision between the Mediterranean Ridge and Calabrian Arc. This combination of processes may re-activate old tectonic features similarly to what has been described by Polonia et alii (2016a) along the Ionian and Alfeo-Etna fault systems. Different tectonics processes are thus acting simultaneously in the study region and

distinguishing the relative contribute of each of them is not trivial. It is not clear, for example, if shortening within the accretionary wedge is still active and if the accretionary wedge is still growing.

5.4 Activity of the CA accretionary wedge and deformation rates

The outermost accretionary wedge and the proto-thrust domains are sites most suitable to record the activity of the Calabrian Arc. In all analysed profiles, the Africa/Eurasia plate boundary, i.e., the outer deformation front, is represented by a fault-controlled anticline bounding the transition between the relatively flat abyssal plain and the accretionary wedge (Figs. 4, 6, 8, 10 and 11). At the toe of the wedge, in the proto-deformation domain, tectonic deformations visible in the MCS lines do not appear reaching up to the seafloor. Moreover, seismo-stratigraphic analyses has shown that an unconformity (Figs. 7a and 9a) is present in the abyssal plain at about 200-250 ms bsf (about 200-250 m), bounding two units with different rates of deformation: high-amplitude folding affects the sediments below the unconformity, while sediments that are more recent show very little deformation. This would imply a slowdown of frontal accretionary processes starting from the age of the unconformity. A Plio-Quaternary unconformity was described also in the inner domains of the accretionary wedge offshore Calabria (Praeg et alii, 2009) and offshore the Messina Straits (Polonia et alii, 2012; 2016a) and interpreted as related to a regional tectonic reorganization. Even though this unconformity represents a transition to lower deformation rates, it is worth noting that the unconformity itself is uplifted and folded close to the deformation front (Fig. 8 s.p. 1600-1700) implying that shortening processes remain active after the unconformity formed, but possibly deformation shifted inwards in the wedge. Moreover, high resolution Chirp data collected in the proto-thrust region (Fig. 9) show that the seafloor is only apparently flat in this region. The HAT deposit, which is the megabed deposited after the AD 365 Crete earthquake and tsunami (Polonia et alii, 2013; 2016b) shows a large wavelength bulge above the fold, at the toe of the accretionary wedge, which might suggest incipient fold growing. The homogenite mud deposit of the megabed,

represented by the transparent unit in Chirp profiles, is generally related to the re-suspension of the finer-grained sediment, which deposit over the basal sand of the turbidite bed (Polonia et alii, 2016c). This homogenite unit could drape pre-existing morphology, implying that the observed seafloor bulge at the toe of the accretionary wedge not necessarily is related to tectonic processes, but rather to the peculiar emplacement process of the megabed. However, Chirp seismic line in Fig. 12b collected along MCS line CALA 04 provide further indications. In this region, the deposition of the HAT produced sediment erosion over the fold (Fig. 12b, ping 2000-3000) while erosion did not take place in the piggy-back basins. This observation suggests that the deposition of the HAT has flattened the topography and thus the observed seafloor bulge has a tectonic origin and post-dates the HAT emplacement time.

Regional ^{14}C dating of the HAT indicates that it was deposited during a single basin-wide event within the time window AD 364–415 and thus it can be traced back to the large tsunami sourced from the AD 365 Crete megathrust earthquake (Polonia et alii 2016b) implying it is about 1650 yrs old.

The HAT uplift above the growing fold is between 2.0-2.5 m suggesting an uplift rate of about 1.1-1.5 mm/yr. This procedure could be applied also to the older megabeds, such as the DDL of Hieke (2000), which is about 14.000 years old (Polonia et alii, 2013). The uplift rate estimated considering the DDL varies between 0.25 and 0.48 mm/year (Fig. 12), but this rate does not take into account sediment compaction. These results suggest that the CA front of the accretionary wedge is still active even though the system is close to continental collision and affected by different transtensional processes orthogonal to the trench axis. An estimate of cumulative tilting of the megabeds in the proto-thrust area (Fig. 13) confirms this interpretation, and suggests the presence of growing folds in the abyssal plain, which are going to incorporate these sediments into the accretionary wedge through frontal accretion. Our data thus suggest that the unconformity within the Plio-Quaternary sediments may be interpreted as a discontinuity in sedimentation and

tectonic development (i.e. a slowdown of shortening rate or an increase in sedimentation rate) but not a real stop in frontal accretion.

Conclusion

We used a multi-scale marine geophysical dataset to describe the tectonic setting of the frontal part of the Calabrian Arc, along the African-Eurasian plate boundary in the Ionian Sea. Several structural domains were described through analysis of multi-channel seismic lines, while a kinematic reconstruction was based on morpho-structural and stratigraphic constraints provided by Chirp-sonar data and morphobathymetric maps. The migrating Calabria trench drives the entire accretionary wedge outward, but the two lobes of the wedge experience different boundary conditions: the eastern lobe (EL) collides with the Mediterranean Ridge and produces basement-involved tectonics, whereas the western lobe (WL) is free to spread into the abyssal plain of the Ionian Sea through frontal accretion and offscraping processes. We found that:

-The WL shows a progression of morphotectonic domains whose structural style and deformation rates varies across strike; the boundaries of such domains are linked to deep faults within the lower plate, suggesting that structural development in the shallow accretionary wedge is driven by inherited structures of the African plate. These structures could represent oceanic fracture zones or paleo-oceanographic boundaries of the Tethyan domain, which presently accommodate intraplate deformation and/or a plate boundary re-organization.

-Seismo-stratigraphic analysis reveals that transtensional faulting along the Alfeo-Etna fault system (AEF) is not very active in the frontal part of the accretionary wedge; the fault is propagating to the SE but deformation rates are low south of the Alfeo seamount.

-Despite rifting processes orthogonal to the trench axis were described in the WL, our data suggest that shortening is active in the proto-deformation zone at the toe of the accretionary wedge. Deformed turbidite beds filling the abyssal plain and perched basins of the accretionary wedge, were used to estimate uplift rates along single folds. Using the two more recent megabeds (the HAT

and DTL) emplaced 1.7 and 14 kyrs b.p., we estimated an uplift rate along the frontal fold of about 0.25-1.5 mm/yr during the Holocene.

-Seismo-stratigraphic analysis has shown that an unconformity is present in the abyssal plain at about 200-250 ms bsf (about 200m). This unconformity, located within Plio-Quaternary (P-Q) deposits, bounds two units with different rates of deformation; high-amplitude folding affects the sediments below the unconformity, while very little deformation is visible above. This would imply a slowdown of frontal accretion starting from the age of the unconformity. The presence of a P-Q event in other domains of the Calabrian Arc points for a regional importance of such unconformity.

- Even though this Plio-Quaternary unconformity represents a transition to lower deformation rates, it is worth noting that the unconformity itself is uplifted and folded close to the deformation front implying that shortening processes remain active, but possibly deformation shifted inwards in the wedge or slowed down.

- We propose that recent structural development in the frontal accretionary wedge is related to a positive flower structure, which is the result of multiple tectonic processes involving Africa/Eurasia plate convergence and lower plate topography entering the subduction complex.

We can conclude that in the incipient collisional setting of the Calabrian Arc deformation patterns are more complex than in classic subduction systems. Morphotectonic processes are strongly dependent on regional aspects concerning large-scale plate motion, such as plate boundary setting, structure of the lower plate, and interference of the two facing and opposite verging Calabrian and Hellenic Arcs and their structural boundaries (i.e. the Ionian and Kephalonia faults). Further studies addressing the recent kinematics of this region and modelling of deformation patterns should focus on these important regional tectonic lineaments.

Acknowledgements
We thank Giuliano Brancolini for seismic line MS-112 and Daniela Accettella for her help in multibeam data processing. Chirp data processing and structural mapping was performed using the open software SeisPrho (Gasperini and Stanghellini, 2009), freely available at http://software.bo.ismar.cnr.it/seisprho. We thank the Editor W. Cavazza and the reviewers P.

Vannucchi and F. Speranza for their comments, which have contributed to improve the manuscript. ISMAR contribution n. 1898.

This work is dedicated to Giovanni Bortoluzzi who died recently. His skill and scientific curiosity in different fields of marine geology have stimulated many multidisciplinary researches in the Istituto di Geologia Marina (now Institute of Marine Sciences, ISMAR) in Bologna. He organized tens of cruises in the Mediterranean Sea and other oceans and dedicated his life to training students and foster collaborative research among colleagues in different disciplines from marine geology, geophysics, biochemistry and oceanography. The acquisition of geophysical data in the Ionian Sea was possible thanks to his valuable contribute. We all miss you Giovanni.

References

ARGNANI A. (2009) - *Evolution of the southern Tyrrhenian slab tear and active tectonics along the western edge of the Tyrrhenian subducted slab*. Geological Society, London, Special Publications, **311**, 193-212, doi:10.1144/SP311.7

BARBERI G., COSENTINO M.T., GERVASI A., GUERRA I., NERI G., AND ORECCHIO B. (2004) - *Crustal seismic tomography in the Calabrian Arc region, south Italy*. Physics of the Earth and Planetary Interiors, **147**, 297–314, doi:10.1016/j.pepi.2004.04.005.

BONARDI G., CAVAZZA W., PERUARONE V., & ROSSI S. (2001) - *Calabria-Peloritani terrane and northern Ionian Sea, in Anatomy of an Orogen: The Apennines and Adjacent Mediterranean Basins*, edited by G. B. Vai and I. P. Martini, Kluwer Academic, Dordrecht, Netherlands, 286–306.

BRADLEY K. E., VASSILAKIS E., HOSA A., & WEISS B. P. (2013) - *Segmentation of the Hellenides recorded by Pliocene initiation of clockwise block rotation in Central Greece*. Earth Planet. Sci. Lett., **362**, 6–19.

CAMERLENGHI A., & CITA M.B., (1987) - *Setting and tectonic evolution of some Eastern Mediterranean deep-sea basins*. Marine Geology, **75**, 31-56.

CERNOBORI L., HIRN A., MCBRIDE J. H., NICOLICH R., PETRONIO L., ROMANELLI M., AND STREAMERS/PROFILES WORKING GROUPS (1996) - *Crustal image of the Ionian basin and its Calabrian margins*. Tectonophysics, 264, 175–189, doi:10.1016/S0040-1951(96)00125-4.

D'AGOSTINO N., AVALLONE A., CHELONI D., D'ANASTASIO E., MANTENUTO S., AND SELVAGGI G. (2008) - *Active tectonics of the Adriatic region from GPS and earthquake slip vectors*. J. Geophys. Res., **113**, B12413, doi:10.1029/2008JB005860.

DEMETS C., GORDON R.G., ARGUS D.F., STEIN S. (1994) - *Effect of recent revisions to the geomagnetic reversal time scale on estimates of current plate motions*. Geophysical research letters **21** (20), 2191-2194

DEVOTI R., RIGUZZI F., CUFFARO M., DOGLIONI C. (2008) - *New GPS constraints on the kinematics of the Apennines subduction*. Earth and Planetary Science Letters, **273**, 163–174

DOGLIONI, C., MERLINI S., AND CANTARELLA G. (1999) - *Foredeep geometries at the front of the Apennines in the Ionian Sea (central Mediterranean)*. Earth Planet. Sci. Lett., **168**, 243–254, doi:10.1016/S0012-821X(99)00059-X.

DOGLIONI C., HARABAGLIA P., MERLINI S., MONGELLI F., PECCERILLO A., PIROMALLO C. (1999b) - *Orogens and slabs vs their direction of subduction*. Earth-Science Reviews, **45**, 167–208.

DOGLIONI, C., INNOCENTI F., & MARIOTTI G. (2001) - *Why Mt Etna?* Terra Nova, **13**(1), 25–31, doi:10.1046/j.1365-3121.2001.00301.x.

FACCENNA, C., BECKER T. W., LUCENTE F. P., JOLIVET L., & ROSSETTI F. (2001a) - *History of subduction and back-arc extension in the central Mediterranean*. Geophys. J. Int., **145**, 809–820, doi:10.1046/j.0956-540x.2001.01435.x.

FACCENNA C., FUNICIELLO F., GIARDINI D., & LUCENTE P. (2001b) - *Episodic back-arc extension during restricted mantle convection in the Central Mediterranean*. Earth and Planetary Science Letters, **187** (1–2), 105–116, DOI: 10.1016/S0012-821X(01)00280-1.

FACCENNA C., PIROMALLO C., CRESPO-BLANC A., JOLIVET L., AND ROSSETTI F. (2004) - *Lateral slab deformation and the origin of the western Mediterranean arcs*. Tectonics, **23**, TC1012, doi:10.1029/2002TC001488.

FACCENNA C., MOLIN P., ORECCHIO B., OLIVETTI V., BELLIER O., FUNICIELLO F., MINELLI L., PIROMALLO C., & BILLI A. (2011) - T*opography of the Calabria subduction zone (southern Italy): Clues for the origin of Mt. Etna*. Tectonics, **30**, TC1003, doi:10.1029/2010TC002694.

FINETTI I.R., LENTINI F., CARBONE S., DEL BEN A., DI STEFANO A., FORLIN E., GUARNIERI P., PIPAN M., & PRIZZON A. (2005) - *Geological outline of Sicily and lithospheric tectono-dynamics of its Tyrrhenian margin from new CROP seismic data*, in: Finetti, I.R. (Ed.), CROP Project: Deep seismic exploration of the Central Mediterranean and Italy, Elsevier, Amsterdam, pp. 319–375.

FRIZON DE LAMOTTE D., RAULIN C., MOUCHOT N., WROBEL-DAVEAU J.-C., BLANPIED C., & RINGENBACH J.-C. (2011) - *The southernmost margin of the Tethys realm during the Mesozoic and Cenozoic: initial geometry and timing of the inversion processes*. Tectonics, **30**, 1–22 TC3002, http://dx.doi.org/10.1029/2010TC002691.

GALLAIS F., GRAINDORGE D., GUTSCHER M.-A., & KLAESCHEN D. (2013) - *Propagation of a lithospheric tear fault (STEP) through the western boundary of the Calabrian accretionary wedge offshore eastern Sicily (Southern Italy)*. Tectonophysics, **602**, 141–152

GALLAIS F., GUTSCHER M. A., KLAESCHEN D., & GRAINDORGE D. (2012) - *Two-stage growth of the Calabrian accretionary wedge in the Ionian Sea (Central Mediterranean): Constraints from depth-migrated multichannel seismic data*. Marine Geology, **326–328**, 28–45, http://dx.doi.org/10.1016/j.margeo.2012.08.006

GASPERINI L., & STANGHELLINI G. (2009) - *SeisPrho: An interactive com- puter program for processing and interpretation of high-resolution seis- mic reflection profiles*. Comput. Geosci., **35**, 1497–1507, doi:10.1016/j.cageo.2008.04.014.

GOES, S., GIARDINI D., JENNY S., HOLLENSTEIN C., KAHLE H.-G., & GEIGER A. (2004) - *A recent tectonic reorganization in the south-central Mediterranean*. Earth Planet. Sci. Lett., **226**, 335–345, doi:10.1016/j.epsl.2004.07.038.

GUEGUEN E., DOGLIONI C., & FERNANDEZ M. (1998) - *On the post-25 Ma geodynamic evolution of the western Mediterranean, Tectonophysics*. **298**, 259–269, doi:10.1016/S0040-1951(98)00189-9.

GUTSCHER M.-A., DOMINGUEZ S., MERCIER DE LEPINAY B., PINHEIRO L., GALLAIS F., BABONNEAU N., CATTANEO A., LE FAOU Y., BARRECA G., MICALLEF A., & ROVERE M. (2016) - *Tectonic expression of an active slab tear from high-resolution seismic and bathymetric data offshore Sicily (Ionian Sea)*. Tectonics, **35**, 39–54, doi:10.1002/2015TC003898.

GVIRTZMAN Z., & NUR A. (1999) - *The formation of Mount Etna as the consequence of slab rollback*. Nature, **401**, 782–785, doi:10.1038/44555.

HERSEY J.B., (1965) - *Sedimentary basins of the Mediterranean Sea*. In: Whitard W.F., Bradshaw W. (eds) Submarine Geology and Geophysics. Proceedings of the 17th Symposium of the Colston Research Society, London. Butterworths, London, 75–91.

HIEKE W. & WERNER F. (2000) - *The Augias megaturbidite in the central Ionian Sea (central Mediterranean) and its relation to the Holocene Santorini event*. Sediment. Geol. **135**, 205 – 218.

HINZ K. (1972) - *Zum Diapirismus im westlichen Mittelmeer*. Geol. Jahrbuch, **90**, 389–396.

HOLLENSTEIN CH., KAHLE H.-G., GEIGER A., JENNY S., GOES S., & GIARDINI D. (2003) - *New GPS constraints on the Africa-Eurasia plate boundary zone in southern Italy*. Geophys. Res. Lett., **30**, 1935, doi:10.1029/2003GL017554, 18.

KASTENS K. A. (1981) - *Structural causes and sedimentological effects of "cobblestone" topography in the eastern Mediterranean Sea*, Ph.D. thesis, Scripps Inst. of Oceanogr., La Jolla, Calif.

KASTENS K. A. & CITA M. B. (1981) - *Tsunami induced sediment transport in the abyssal Mediterranean Sea*. Geol. Soc. Am. Bull., **89**, 591–604.

JOLIVET L. & FACCENNA C. (2000) - *Mediterranean extension and the Africa-Eurasia collision*. Tectonics, **19**, 1095–1106, doi:10.1029/2000TC900018.

LALLEMAND S. E., MALAVIEILLE J. & CALASSOU S. (1992). *Effects of oceanic ridge subduction on accretionary wedges: Experimental modeling and marine observations*. Tectonics, **11** (6), 1301–1313. doi: 10.1029/92TC00637.

MALINVERNO A. & RYAN W. B. F. (1986) - *Extension in the Tyrrhenian Sea and shortening in the Apennines as result of arc migration driven by sinking of the lithosphere*. Tectonics, **5**, 227–245, doi:10.1029/TC005i002p00227.

MARANI M. P. & TRUA T. (2002) - *Thermal constriction and slab tearing at the origin of a superinflated spreading ridge: Marsili volcano (Tyrrhenian Sea)*. J. Geophys. Res., **107**(B9), 2188, doi:10.1029/2001JB000285.

MATTEI M., CIFELLI F. & D'AGOSTINO N. (2007). *The evolution of the Calabrian Arc: Evidence from paleomagnetic and GPS observations*. Earth and Planetary Science Letters, **263**, 259–274. doi:10.1016/j.epsl.2007.08.034.

MATTEI M., CIPOLLARI P., COSENTINO D., ARGENTIERI A., ROSSETTI F., SPERANZA F., & DI BELLA L. (2002). *The Miocene tectono-sedimentary evolution of the Southern Tyrrhenian Sea: stratigraphy, structural and paleomagnetic data from the on-shore Amantea basin (Calabrian arc, Italy)*. Basin Research, **14**, 147-168. doi:10.1046/j.1365-2117.2002.00173.x.

MINELLI L. & FACCENNA C. (2010) - *Evolution of the Calabrian accretionary wedge (central Mediterranean)*. Tectonics, **29**, TC4004, doi:10.1029/2009TC002562.

NICOLICH R., LAIGLE M., HIRN A., CERNOBORI L., & GALLART J. (2000) - *Crustal structure of the ionian margin of Sicily: Etna volcano in the frame of regional evolution*. Tectonophysics, **329**, 121-139, doi:10.1016/S0040-1951(00)00192-X.

NICOLOSI I., SPERANZA F., & CHIAPPINI M. (2006) - *Ultrafast oceanic spreading of the Marsili Basin, southern Tyrrhenian Sea: Evidence from magnetic anomaly analysis*. Geology, **34**(9), 717-720, doi: 10.1130/G22555.1.

PATACCA E., SARTORI R., & SCANDONE P. (1990) - *Tyrrhenian basin and Apenninic arcs: Kinematic relation since Late Tortonian times*. Mem. Soc. Geol. Ital., **45**, 425–451.

POLONIA, A., TORELLI L., MUSSONI P., GASPERINI L., ARTONI A., & KLAESCHEN D. (2011) - *The Calabrian Arc subduction complex in the Ionian Sea: Regional architecture, active deformation, and seismic hazard*. Tectonics, **30**, TC5018, doi:10.1029/2010TC002821.

POLONIA A., TORELLI L., GASPERINI L., & MUSSONI P. (2012) - *Active faults and historical earthquakes in the Messina Straits area (Ionian Sea)*. Nat. Hazards Earth Syst. Sci., **12**, 2311-2328, doi:10.5194/nhess-12-2311-2012.

POLONIA A., TORELLI L., ARTONI A., CARLINI M., FACCENNA C., FERRANTI L., GASPERINI L., GOVERS R., KLAESCHEN D., MONACO C., NERI G., NIJHOLT N., ORECCHIO B., & WORTEL R. (2016a) - *The Ionian and Alfeo-Etna fault zones: new segments of an evolving plate boundary in the central mediterranean sea?* Tectonophysics, **675**, 69-90. doi:10.1016/j.tecto.2016.03.016

POLONIA A., VAIANI S.C., DE LANGE G.J. (2016b) - *Did the A.D. 365 Crete earthquake/tsunami trigger synchronous giant turbidity currents in the Mediterranean Sea?* Geology, **44** (3), 191-194. DOI: 10.1130/G37486.1

POLONIA A., BONATTI E., CAMERLENGHI A., LUCCHI R. G., PANIERI G., & GASPERINI L. (2013) - *Mediterranean megaturbidite triggered by the AD 365 Crete earthquake and tsunami*. Scientific Reports, **3**, 1285, DOI: 10.1038/srep01285.

POLONIA A., NELSON H.C., ROMANO S., VAIANI S.C., COLIZZA E., GASPAROTTO G., &, GASPERINI L. (2016c) - *A depositional model of seismo-turbidites in confined basins based on Ionian Sea deposits.* Marine Geology, DOI**:**10.1016/j.margeo.2016.05.010.

PRAEG D., CERAMICOLA S., BARBIERI R., UNNITHAN V., & WARDELL N. (2009) - *Tectonically-driven mud volcanism since the late Pliocene on the Calabrian accretionary prism, central Mediterranean Sea*. Mar. Pet. Geol., **26**, 1849–1865, doi:10.1016/j.marpetgeo.2009.03.008.

REHAULT J.P., BOILLOT G., & MAUFFRET A. (1984) - *The western Mediterranean Basin geological Evolution*. Marine Geology, **55**, 447–477.

ROSENBAUM G. & LISTER G. S. (2004) - *Neogene and Quaternary rollback evolution of the Tyrrhenian Sea, the Apennines, and the Sicilian Maghrebides*. Tectonics, **23**, TC1013, doi:10.1029/2003TC001518.

ROSENBAUM G., LISTER G. S., & DUBOZ C. (2002) - *Reconstruction of the tectonic evolution of the western Mediterranean since the Oligocene*. in G. Rosenbaum and G. S. Lister (Eds.), Reconstruction of the evolution of the Alpine-Himalayan Orogen, Journal of the Virtual Explorer, **8**, 107 - 130.

ROSENBAUM G., GASPARON M., LUCENTE F. P., PECCERILLO A., & MILLER M. S. (2008) - *Kinematics of slab tear faults during subduction segmentation and implications for Italian magmatism*. Tectonics, **27**, TC2008, doi:10.1029/2007TC002143.

ROSSI S. & SARTORI R. (1981) - *A seismic reflection study of the External Calabrian Arc in the northern Ionian Sea (eastern Mediterranean)*. Mar. Geophys. Res., **4**, 403–426. doi:10.1007/BF00286036

ROYDEN L. H. & PAPANIKOLAOU D. J. (2011) - *Slab segmentation and late Cenozoic disruption of the Hellenic arc*. Geochem. Geophys. Geosyst., **12**, Q03010, doi:10.1029/2010GC003280.

RYAN W. B. F., HSÜ, K. J. ET ALII (1973) - *Initial Reports of the Deep Sea Drilling Project*, Government Printing Office, Washington, **13**, 517–1447.

SERPELLONI E., VANNUCCI G., PONDRELLI S., ARGNANI A., CASULA G., ANZIDEI M., BALDI P. AND GASPERINI P. (2007) - *Kinematics of the Western Africa-Eurasia plate boundary from focal mechanisms and GPS data. Geophysical Journal International*. Geophysical Journal International, **169**, 1180–1200. doi: 10.1111/j.1365-246X.2007.03367.x

SPERANZA F., MINELLI L., PIGNATELLI A. AND CHIAPPINI M. (2012) – *The Ionian Sea: the oldest in situ ocean fragment of the world?* Journal of Geophysical Research, **117**, B12101. doi:10.1029/2012JB009475.

WORTEL M. J. R. & SPAKMAN W. (2000) - *Subduction and slab detachment in the Mediterranean-Carpathian region*. Science, **290**, 1910–1917, doi:10.1126/science.290.5498.1910.

Figure Captions

Fig. 1 – Geodynamic setting of the central Mediterranean Sea. Shaded relief map of topography/bathymetry of the central and eastern Mediterranean Sea: Global Bathymetry and Elevation Data from SRTM30_PLUS (Becker et alii, 2009). The geological model is modified from Polonia et alii (2011). Slip vector in the African reference frame is indicated by a yellow arrow. The NW ward dipping subducting slab of the African plate is represented by the yellow isodepth lines in the Tyrrhenian Sea spacing from 100 to 450 Km depth (Selvaggi and Chiarabba, 1995). Eu: Europe, Afr: Africa.

Fig. 2 – Structural map of the CA region derived from integrated interpretation of available seismic data and multibeam bathymetry (modified from Polonia et alii, 2016) superposed over a gray levels bathymetric slope map. Major structural boundaries, active faults and the extent of the structural domains (i.e. pre and post-Messinian wedges and inner plateau) are indicated. The continental margin is segmented both across and along strike. The deformation zones corresponding to the major lithospehric faults segmenting the continental margin (i.e. the Alfeo-Etna and Ionian fault systems) are indicated by the grey pattern. The diffuse structural boundary between EL and WL accommodates different rates of shortening, slab rollback and tearing in the different segments of the CA subduction zone.

Fig. 3 – **a**: Line drawing of the PSDM (Pre Stack Depth Migrated) MCS line CROP M-2B (modified from Polonia et alii, 2011 and 2012) collected in the Western Lobe. **b**: Line drawing of PSDM MCS line CROP M-4 (modified from Polonia et alii, 2011 and 2012) collected in the Eastern Lobe. Location of seismic profiles is shown in Figure 2. Yellow reflector: base of Plio-Quaternary sediments; Orange reflector: base of Messinian evaporites; Green domain: base of Tertiary sediments; and Mesozoic sediments; Purple reflector: African plate basement.

Fig. 4 – Seismic (above) and line drawing (below) of high resolution MCS time migrated line CALA-05 across the western part of the WL close to the Malta escarpment (see Figure 2 for location). Yellow reflector: base of Plio-Quaternary sediments; Orange reflector: base of Messinian evaporites; Green domain: base of Tertiary sediments; and Mesozoic sediments; Purple reflector: African plate basement.

Fig. 5 – a: Zoom of MCS line CALA-05) across the deformation front (location on Figure 4). As the relatively undeformed abyssal plain sediments approach the deformation front they are folded and uplifted and included through frontal accretion in the wedge. b: Chirp seismic line collected in the abyssal plain close to the Malta escarpment (Figure 2 for location). A succession of sediment drifts possibly related to bottom currents are imaged.

Fig. 6 – Seismic (above) and line drawing (below) of high resolution MCS time migrated line CALA-04 across the central part of the WL (see Figure 2 for location). Yellow reflector: base of Plio-Quaternary sediments; Orange reflector: base of Messinian evaporites; Green domain: base of Tertiary sediments; and Mesozoic sediments; Purple reflector: African plate basement.

Fig. 7 - a: Zoom of MCS line CALA-04 across the deformation front (location in Figure 6). A major unconformity at about 200 ms (TWT) is present in the abyssal plain. This unconformity separates sediment packets with different rates of deformation. The unconformity itself as it reaches the outer deformation front is uplifted and deformed. b: Chirp seismic line collected across the outer deformation front. Three major megabeds are well imaged in the abyssal plain (HAT: Homogenite/Augias turbidite; DTL: deep transparent layer; TTL: thick transparent layer).

Fig. 8 - Seismic (above) and line drawing (below) of high resolution MCS time migrated seismic line CALA-15 across the eastern part of the WL (see Figure 2 for location). Yellow reflector: base of Plio-Quaternary sediments; Orange reflector: base of Messinian evaporites; Green domain: base of Tertiary sediments; and Mesozoic sediments; Purple reflector: African plate basement.

Fig. 9 - a: Zoom of MCS line CALA-15 across the deformation front (location on Figure 8). A major unconformity at about 200 ms (TWT) is present in the abyssal plain. This unconformity separates sediment packets with different rates of deformation. The unconformity itself as it reaches the outer deformation front is uplifted and deformed. b: Chirp seismic line collected across the outer deformation front. Three major megabeds are visible in the abyssal plain (HAT: Homogenite/Augias turbidite; DTL: deep transparent layer; TTL: thick transparent layer).

Fig. 10 – Migrated seismic line MS-112 (above) and its line drawing (below) across the WL of the accretionary wedge (see Figure 2 for location). Yellow reflector: base of Plio-Quaternary sediments; Orange reflector: base of Messinian evaporites; Green domain: base of Tertiary sediments; and Mesozoic sediments; Purple reflector: African plate basement. CD: crustal discontinuity.

Fig. 11 – High resolution morphobathymetric map of the frontal part of the WL. Two lateral ramps (LR1 and LR2) offset left-laterally the deformation front. Major structural domains in the frontal accretionary wedge (gentle and tight deformation, rough deformation and highstanding plateau) are characterized by varying morphology on the map.

Fig. 12 – Chirp seismic profile in the proto-thrust area where three megabeds are present (HAT: Homogenite/Augias turbidite; DTL: deep transparent layer; TTL: thick transparent layer). The uplift of the HAT and DTL megabeds, whose age was reconstructed through ^{14}C dating, was used to estimate uplift rates in this area during the Holocene.

Fig. 13 – Chirp seismic profile in the proto-thrust area. An estimate of cumulative tilting of the megabeds HAT, DTL and TTL in the proto-thrust area. Cumulative titling of these reference layers suggests the presence of growing folds in the abyssal plain, which are going to incorporate these sediments into the accretionary wedge through frontal accretion.

Table captions:

Table 1 - Acquisition parameters, processing sequence and resolution of geophysical data used in this study.

Table 2 - depth of principal seismic reflectors in 8 seismic lines (from West to East).

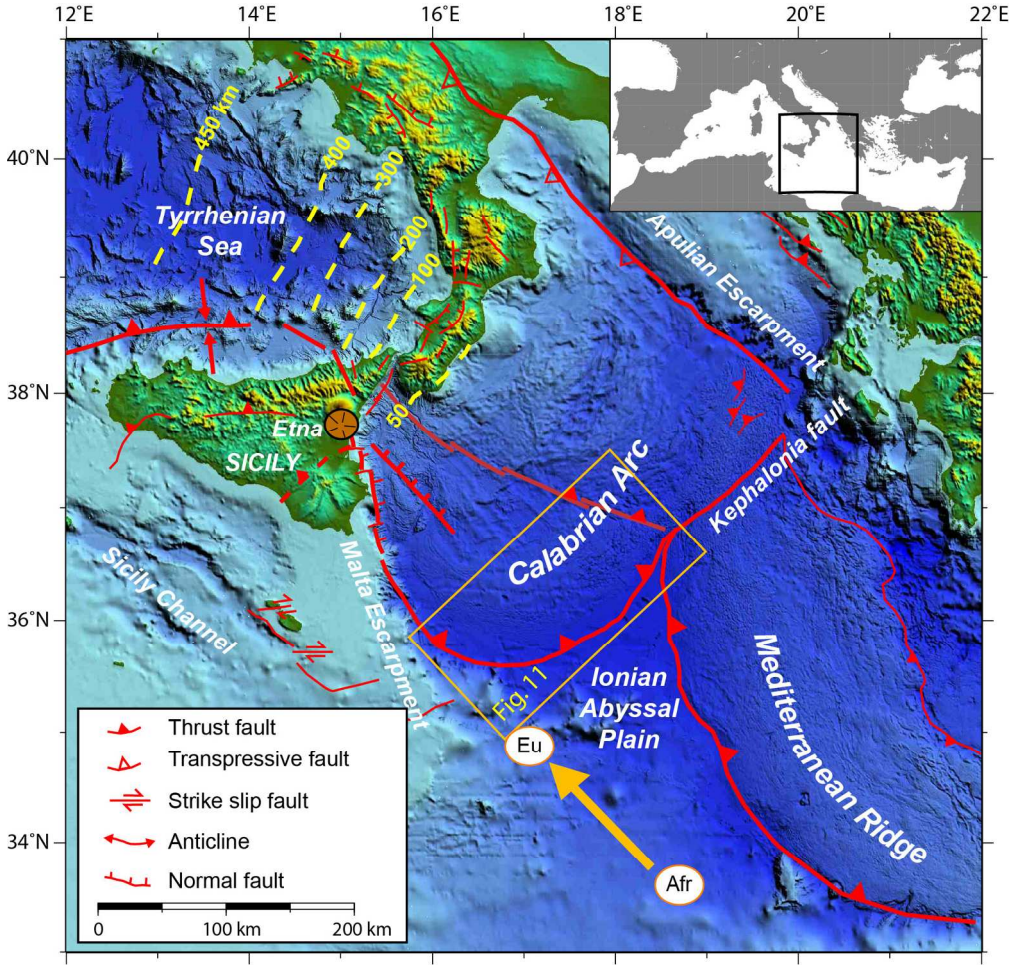

Fig. 1 – Geodynamic setting of the central Mediterranean Sea. Shaded relief map of topography/bathymetry of the central and eastern Mediterranean Sea: Global Bathymetry and Elevation Data from SRTM30_PLUS (Becker et alii, 2009). The geological model is modified from Polonia et alii (2011). Slip vector in the African reference frame is indicated by a yellow arrow. The NW ward dipping subducting slab of the African plate is represented by the yellow isodepth lines in the Tyrrhenian Sea spacing from 100 to 450 Km depth (Selvaggi and Chiarabba, 1995). Eu: Europe, Afr: Africa.

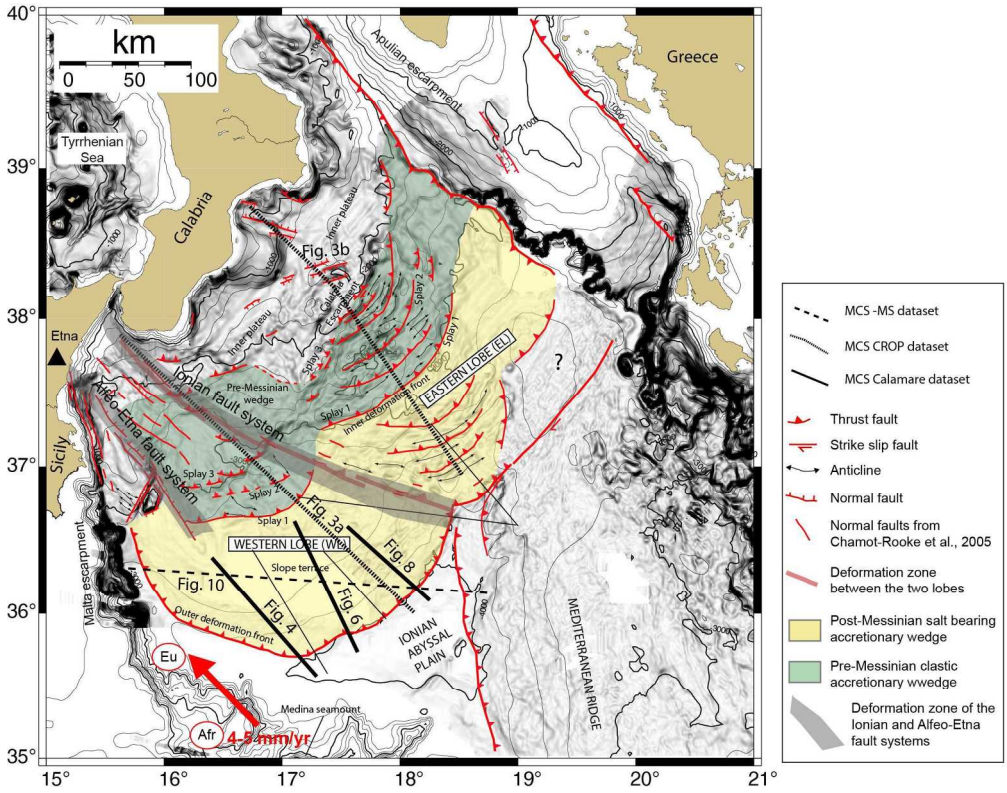

Fig. 2 – Structural map of the CA region derived from integrated interpretation of available seismic data and multibeam bathymetry (modified from Polonia et alii, 2016) superposed over a gray levels bathymetric slope map. Major structural boundaries, active faults and the extent of the structural domains (i.e. pre and post-Messinian wedges and inner plateau) are indicated. The continental margin is segmented both across and along strike. The deformation zones corresponding to the major lithospehric faults segmenting the continental margin (i.e. the Alfeo-Etna and Ionian fault systems) are indicated by the grey pattern. The diffuse structural boundary between EL and WL accommodates different rates of shortening, slab rollback and tearing in the different segments of the CA subduction zone.

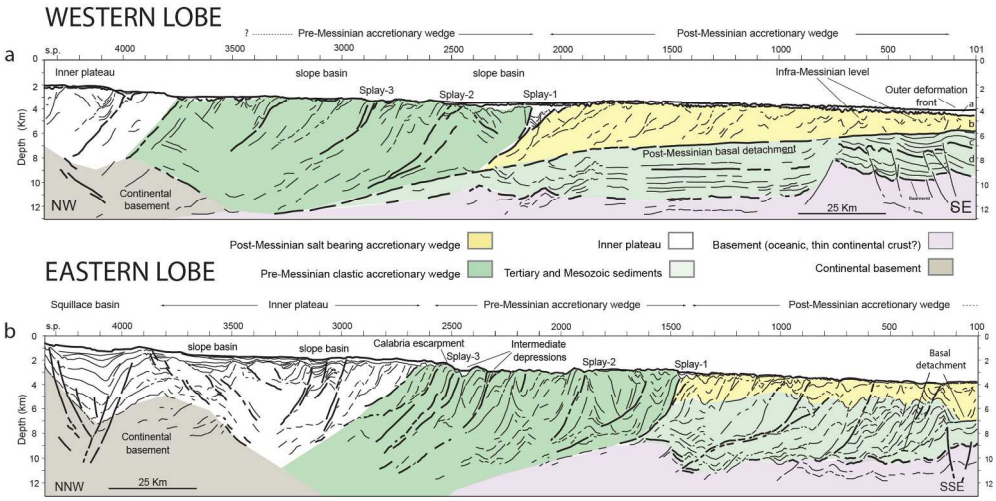

Fig. 3 – a: Line drawing of the PSDM (Pre Stack Depth Migrated) MCS line CROP M-2B (modified from Polonia et alii, 2011 and 2012) collected in the Western Lobe. b: Line drawing of PSDM MCS line CROP M-4 (modified from Polonia et alii, 2011 and 2012) collected in the Eastern Lobe. Location of seismic profiles is shown in Figure 2. Yellow reflector: base of Plio-Quaternary sediments; Orange reflector: base of Messinian evaporites; Green domain: base of Tertiary sediments; and Mesozoic sediments; Purple reflector: African plate basement.

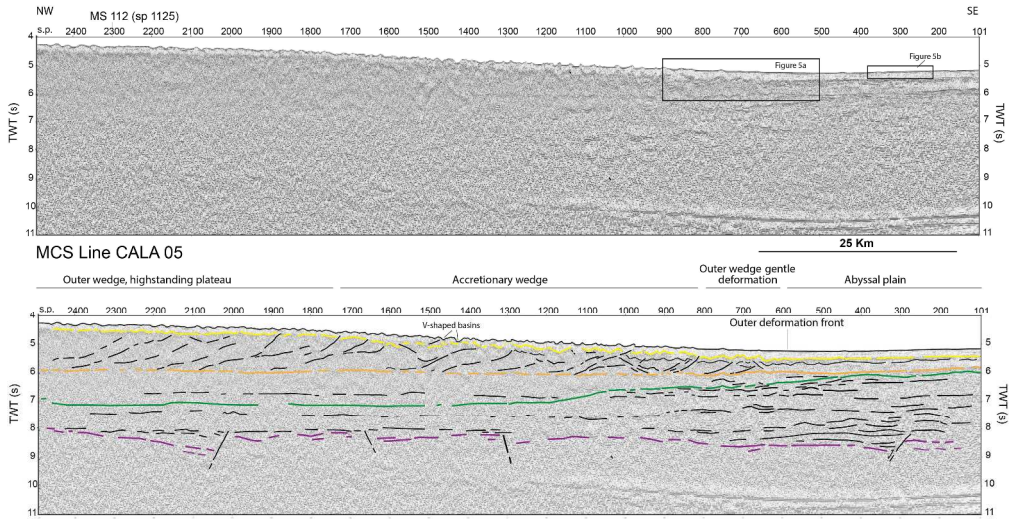

Fig. 4 – Seismic (above) and line drawing (below) of high resolution MCS time migrated line CALA-05 across the western part of the WL close to the Malta escarpment (see Figure 2 for location). Yellow reflector: base of Plio-Quaternary sediments; Orange reflector: base of Messinian evaporites; Green domain: base of Tertiary sediments; and Mesozoic sediments; Purple reflector: African plate basement.

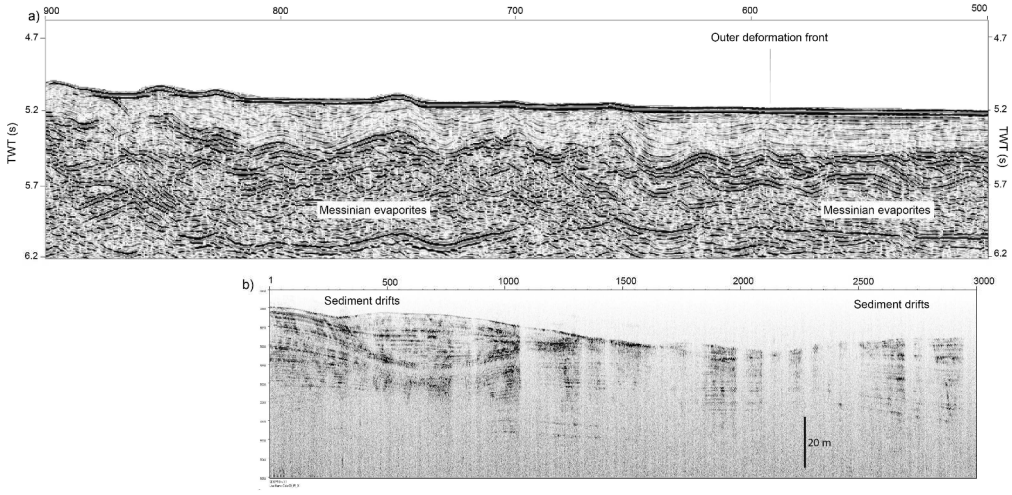

Fig. 5 – a: Zoom of MCS line CALA-05) across the deformation front (location on Figure 4). As the relatively undeformed abyssal plain sediments approach the deformation front they are folded and uplifted and included through frontal accretion in the wedge. b: Chirp seismic line collected in the abyssal plain close to the Malta escarpment (Figure 2 for location). A succession of sediment drifts possibly related to bottom currents are imaged.

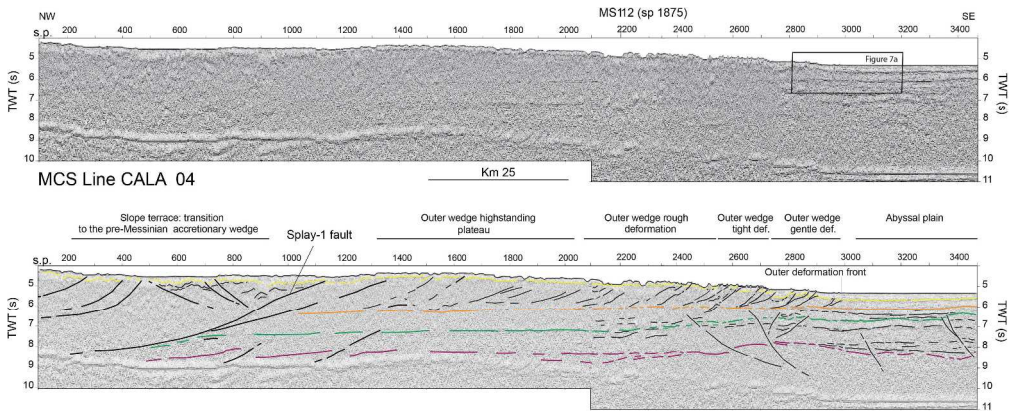

Fig. 6 – Seismic (above) and line drawing (below) of high resolution MCS time migrated line CALA-04 across the central part of the WL (see Figure 2 for location). Yellow reflector: base of Plio-Quaternary sediments; Orange reflector: base of Messinian evaporites; Green domain: base of Tertiary sediments; and Mesozoic sediments; Purple reflector: African plate basement.

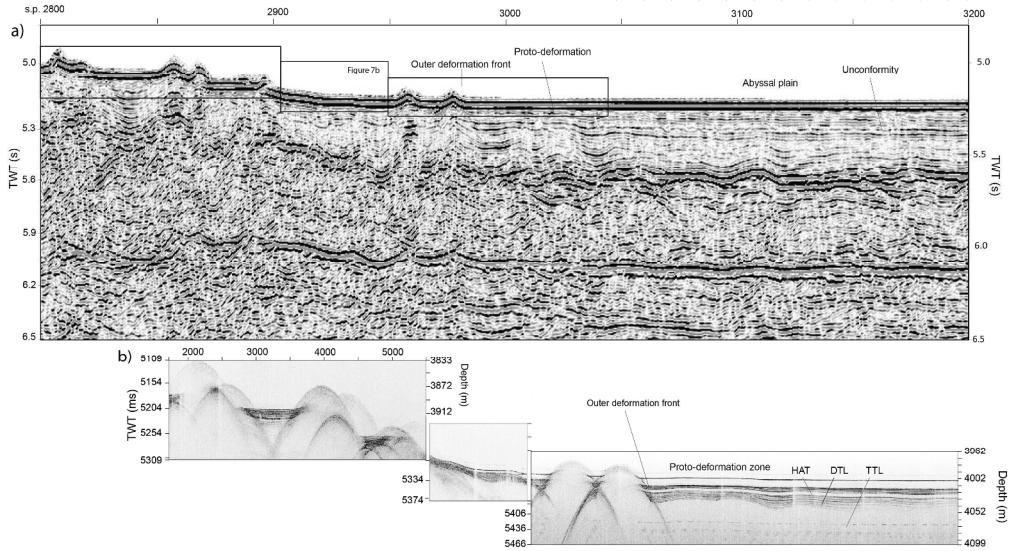

Fig. 7 - a: Zoom of MCS line CALA-04 across the deformation front (location in Figure 6). A major unconformity at about 200 ms (TWT) is present in the abyssal plain. This unconformity separates sediment packets with different rates of deformation. The unconformity itself as it reaches the outer deformation front is uplifted and deformed. b: Chirp seismic line collected across the outer deformation front. Three major megabeds are well imaged in the abyssal plain (HAT: Homogenite/Augias turbidite; DTL: deep transparent layer; TTL: thick transparent layer).

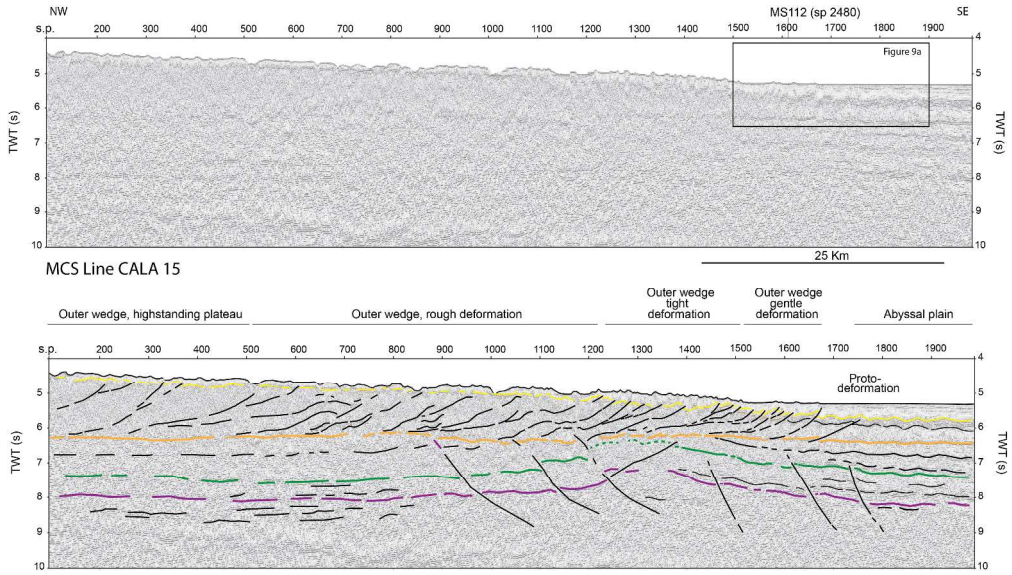

Fig. 8 - Seismic (above) and line drawing (below) of high resolution MCS time migrated seismic line CALA-15 across the eastern part of the WL (see Figure 2 for location). Yellow reflector: base of Plio-Quaternary sediments; Orange reflector: base of Messinian evaporites; Green domain: base of Tertiary sediments; and Mesozoic sediments; Purple reflector: African plate basement.

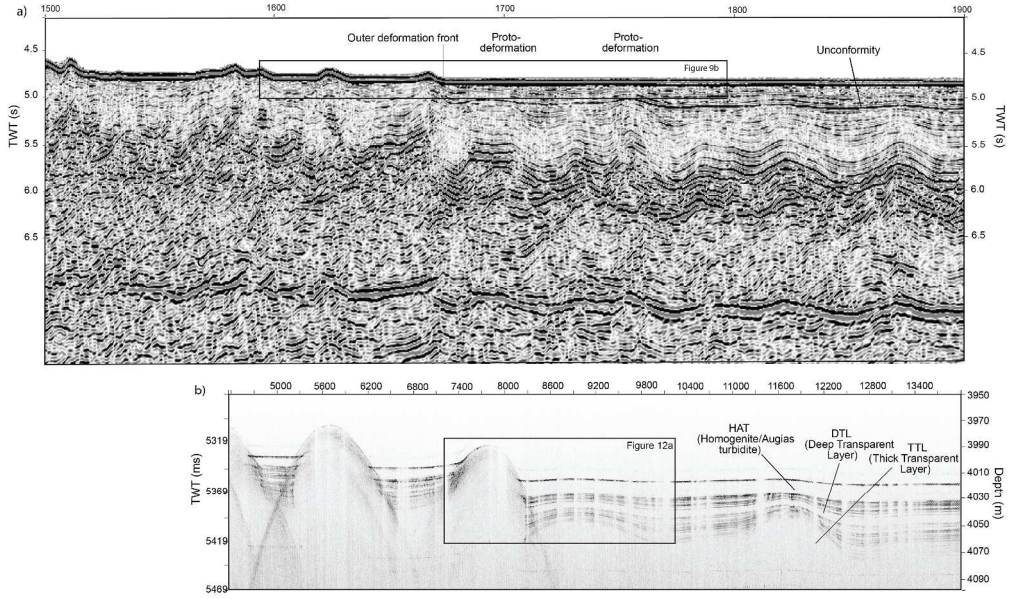

Fig. 9 - a: Zoom of MCS line CALA-15 across the deformation front (location on Figure 8). A major unconformity at about 200 ms (TWT) is present in the abyssal plain. This unconformity separates sediment packets with different rates of deformation. The unconformity itself as it reaches the outer deformation front is uplifted and deformed. b: Chirp seismic line collected across the outer deformation front. Three major megabeds are visible in the abyssal plain (HAT: Homogenite/Augias turbidite; DTL: deep transparent layer; TTL: thick transparent layer).

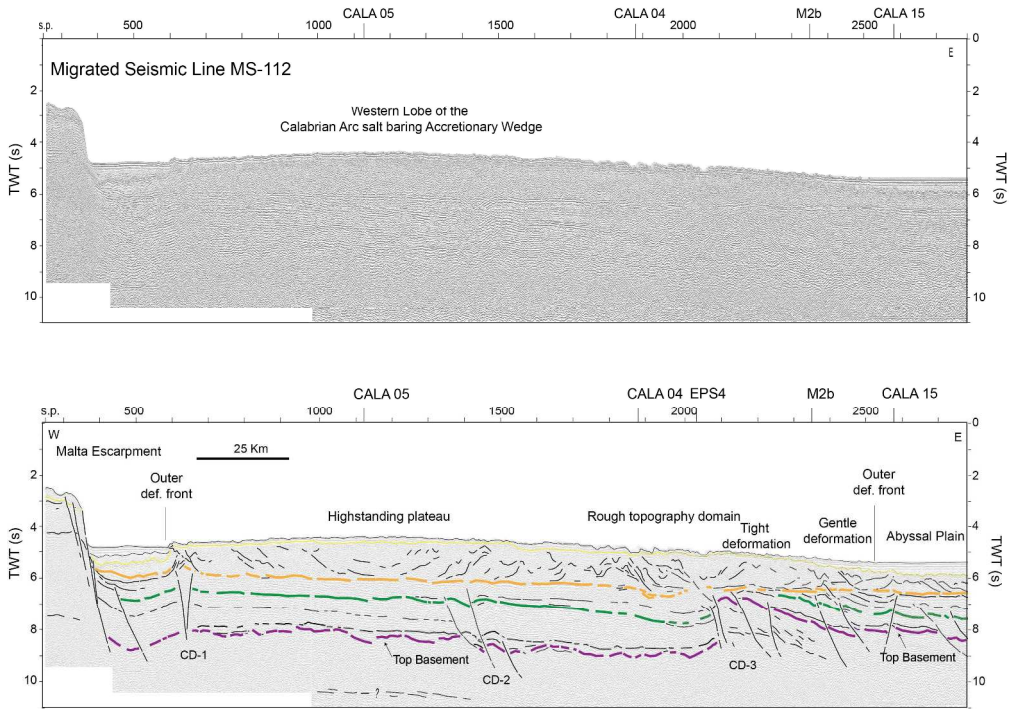

Fig. 10 – Migrated seismic line MS-112 (above) and its line drawing (below) across the WL of the accretionary wedge (see Figure 2 for location). Yellow reflector: base of Plio-Quaternary sediments; Orange reflector: base of Messinian evaporites; Green domain: base of Tertiary sediments; and Mesozoic sediments; Purple reflector: African plate basement. CD: crustal discontinuity.

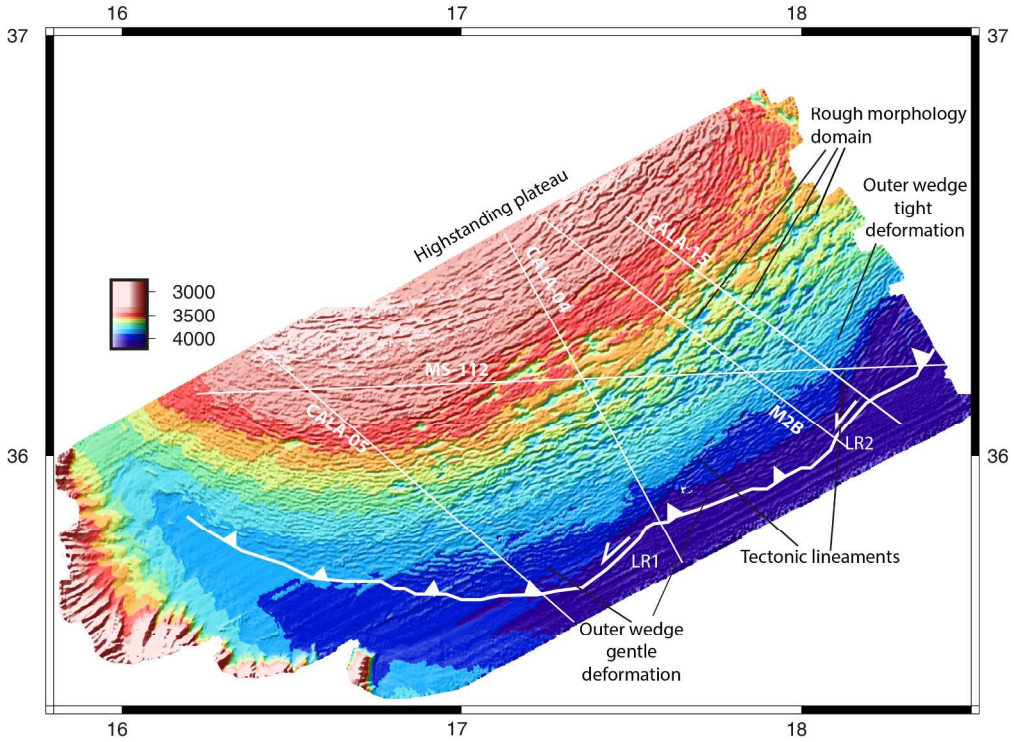

Fig. 11 – High resolution morphobathymetric map of the frontal part of the WL. Two lateral ramps (LR1 and LR2) offset left-laterally the deformation front. Major structural domains in the frontal accretionary wedge (gentle and tight deformation, rough deformation and highstanding plateau) are characterized by varying morphology on the map.

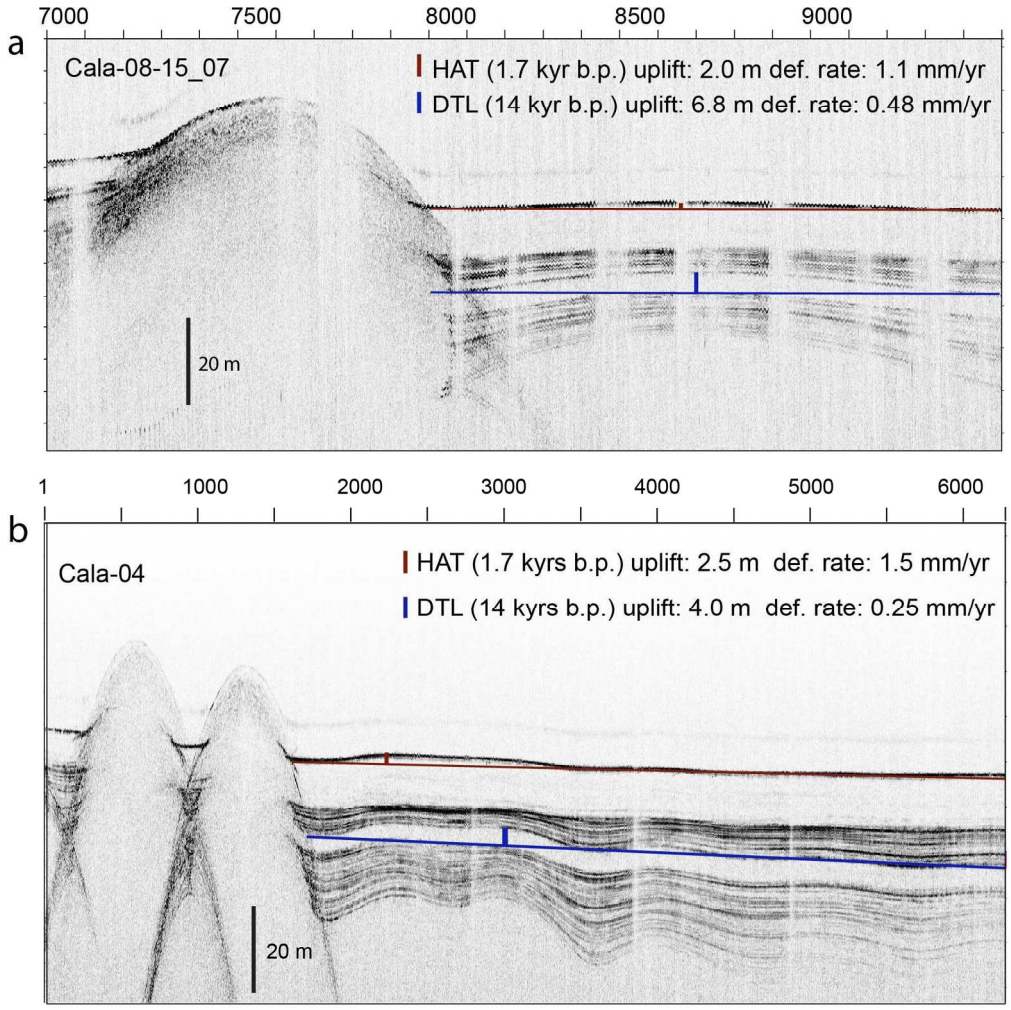

Fig. 12 – Chirp seismic profile in the proto-thrust area where three megabeds are present (HAT: Homogenite/Augias turbidite; DTL: deep transparent layer; TTL: thick transparent layer). The uplift of the HAT and DTL megabeds, whose age was reconstructed through 14C dating, was used to estimate uplift rates in this area during the Holocene.

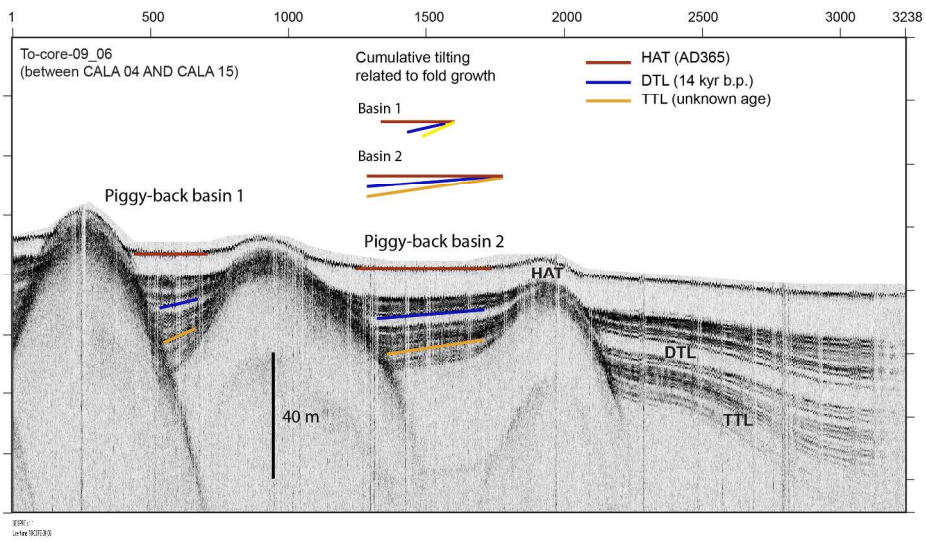

Fig. 13 – Chirp seismic profile in the proto-thrust area. An estimate of cumulative tilting of the megabeds HAT, DTL and TTL in the proto-thrust area. Cumulative titling of these reference layers suggests the presence of growing folds in the abyssal plain, which are going to incorporate these sediments into the accretionary wedge through frontal accretion.

GEOPHYSICAL MULTI-SCALE DATASET	Acquisition parameters	Main processing sequence
Deep penetration MCS (CROP dataset)	Source: 4906 cu inch air guns Streamer: 4500 m Group interval: 25 m Shot Interval: 62.5 m Coverage: 3600% Sampl. Int.: 4 msec	Full pre-stack depth-migration (PSDM), with SIRIUS/GXT, Migpack software package.
Deep penetration MCS (MS dataset)	Source: 4906 cu inch air guns Streamer: 4500 m Group interval: 25 m Shot Interval: 62.5 m Coverage: 3600% Sampl. Int.: 4 msec	Preliminary velocity analysis, Dip Move Out (DMO), velocity analysis after DMO, stack and time migration
High resolution MCS seismic (CALAMARE)	Source: 2 Sodera G.I. guns, Streamer: 600 m Group int.: 12.5 m Shot interval: 50 m Coverage: 600% Sampl. Int.: 1 msec	Velocity analysis, stack, DMO, velocity analysis, stack
Sub-bottom Seismic data	16 hull mounted transducers CHIRP-Benthos sonar system (3-7 KHz sweep frequency)	Data represented through variable density section with instantaneous amplitude
Multibeam data	Reson 8150	100 m grid

Table 1 – Acquisition parameters, processing sequence and resolution of geophysical data used in this study

MCS line	Base Messinian	K reflector	Basement (high)
Cala-05	5,8 sec	6,0 sec	8,2 sec (no high)
Cala-13	5,8 sec	6,0 sec	8,1 sec (no high)
MS-27	5,8 sec	6,0 sec	8,2 sec (no high)
Cala-04	6,0 sec	6,4 sec	8,2 sec (7,8 sec)
PM-01	6,0 sec	7,0 sec	8,2 sec (7,3 sec)
Cala-14	6,4 sec	7,2 sec	8,4 sec (7,2 sec)
M-2B	6,2 sec	7,2 sec	8,2 sec (7.7 sec)
Cala 15	6,5 sec	7,4 sec	8,2 sec (7,4 sec)

Table 2 - depth of principal seismic reflectors in 8 seismic lines (from West to East).